

# Lecture 4

## Plasma waves II

### 4.1 Aims and Learning Outcomes

The **Aim** of this lecture is to explore how waves and electromagnetic radiation grow and damp. This allows the knowledge of wave modes developed in previous lectures to be applied in the contexts discussed in the rest of the course.

**Expected Learning Outcomes.** You are expected to be able to

- Understand and be able to explain the physics of Landau damping and wave growth via inverse Landau damping.
- Follow the derivations of Landau damping for Langmuir and transverse (free-space) waves.
- Understand and explain the concepts and connections between wave instabilities, quasilinear relaxation, back-reaction to the wave growth, and marginal stability.
- Explain qualitatively several reasons why waves grow in bursts in realistic plasmas.
- Understand the origin of nonlinear wave processes and be able to list some of their consequences.
- Explain these ideas for type III solar radio bursts and be able to apply them qualitatively to analogous phenomena.

### 4.2 Qualitative physics of Landau damping and inverse Landau damping

Consider an electrostatic wave with frequency  $\omega$  and wavevector  $\mathbf{k}$ . Recall from Lecture 3 that there is a singularity in the dielectric tensor (3.23) where

$$\omega - \mathbf{k} \cdot \mathbf{v} = 0. \quad (4.1)$$

This is the condition for resonance between particles and waves in an unmagnetized plasma, where the component of the particle velocity  $\mathbf{v}$  parallel to  $\mathbf{k}$  is equal to the phase velocity of the wave  $v_\phi = \omega/k$ . After Lorentz transforming to the frame where the particle is at rest (with frequency  $\omega'$  and wavevector  $\mathbf{k}'$  in the rest frame), we find

$$\omega' = \gamma(\omega - \mathbf{k} \cdot \mathbf{v}), \quad (4.2)$$

where  $\gamma$  is the Lorentz factor of the particle. When the resonance condition (4.1) is satisfied, it follows that  $\omega' = 0$ ; i.e., the electric field of the waves appears static (but varying periodically in space) in the rest frame of the particle. Equivalently we can Lorentz transform into a frame in which the wave field is static in time but varies periodically with position (the “wave frame”).

A particle that is initially at rest at location  $x$  in the wave frame is accelerated by the static electric field unless  $E(x) = 0$ , so that energy is transferred from the waves to the particle. However, the periodic nature of the electric field means that no energy is exchanged when averaged over a cycle. A particle that is not initially at rest in the wave frame will also move through the static wave field exchanging energy. A detailed perturbation analysis of the particle motion in the wave field [Melrose, 1986, Chapter 5] shows that to zeroth and first order (in the field amplitude) there is no energy exchange in the time-asymptotic limit. However, there is a non-zero energy exchange at second order. One can show that particles travelling slightly slower than the resonance velocity ( $v \lesssim v_\phi$ ) see a nearly static electric field which acts to “drag” them towards the resonance velocity. This acceleration of particles is associated with a transfer of energy from the waves to the particles; in other words, this corresponds to damping of the waves. Similarly, particles travelling slightly faster than the resonance velocity ( $v \gtrsim v_\phi$ ) are decelerated to the resonance velocity. In this case, energy is transferred from the particles to the waves and so the waves grow in amplitude.

Whether a wave grows or damps then depends on whether there are more or fewer particles at speeds above the wave phase speed than below the wave phase speed. The essential ingredient that leads to Landau damping is that the slope of the equilibrium (Maxwellian) distribution function at the resonance velocity is negative. As illustrated in Figure 4.1, there are more particles accelerated towards  $v = v_\phi$  from below than from above, leading to a net transfer of energy from the waves to the particles.

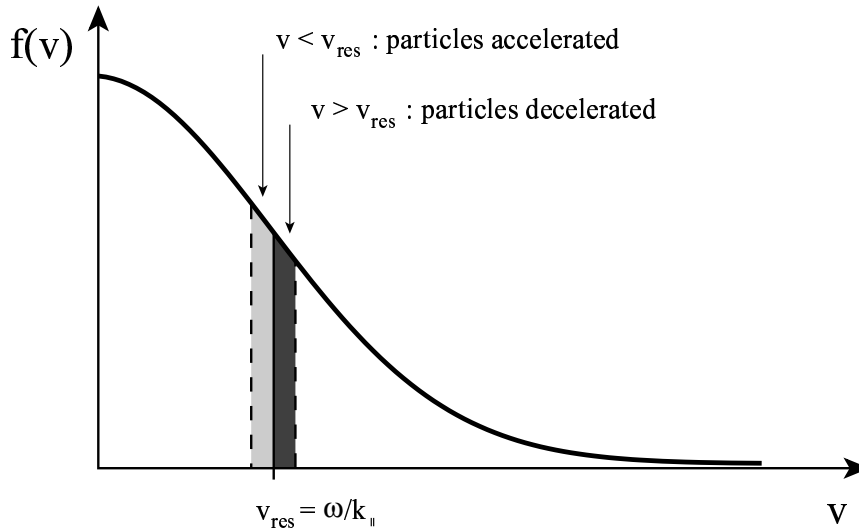


Figure 4.1: Landau damping - more particles below the resonance velocity are dragged into resonance than above, because of the negative slope in the Maxwellian particle distribution, leading to a net flow of energy to the resonant particles.

What happens if the gradient  $\partial f/\partial v > 0$  at  $v = v_\phi$ ? Then the waves grow since there are more particles losing energy near  $v_\phi$  than gaining energy. This situation is illustrated in Figure 4.2 below. Thus, the inverse of Landau damping is wave

growth. This is an example of the maxims of Einstein and Kirchoff that for every absorption (damping) process there is an emission process.

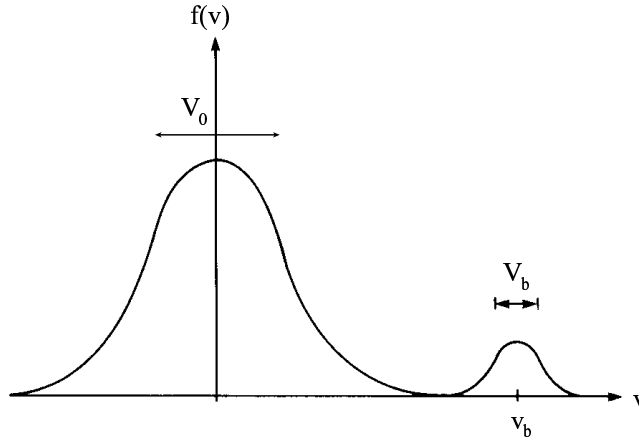


Figure 4.2: Distribution function consisting of a Maxwellian and a beam.

It is emphasized that Landau damping is a collisionless damping mechanism - it does not involve Coulomb interactions between particles in a plasma or other collisions.

### 4.3 Mathematical details for Landau damping

A mathematical expression for Landau damping is obtained by allowing the wave frequency  $\omega$  to have a small imaginary part  $i\omega_i$  (with  $\omega_i \ll \omega_r$ ) for real wavevector  $\mathbf{k}$ , substituting these into the dispersion equation (3.16), and retaining the imaginary part of the dielectric tensor. The wave amplitude then varies as  $\exp[\omega_i t]$ , and hence the imaginary part contributes to wave damping (or growth).

Consider, as an example, the dispersion equation for electrostatic waves,

$$K_L(\omega, \mathbf{k}) = 0 . \quad (4.3)$$

Dividing  $K_L$  into real (Re) and imaginary (Im) parts and Taylor expanding about  $\omega = \omega_r$  this equation becomes

$$Re[K_L(\omega_r)] + i\omega_i \frac{\partial}{\partial \omega_r} Re[K_L(\omega_r)] + iIm[K_L(\omega_r)] + i \frac{\partial}{\partial \omega_r} (Im[K_L(\omega_r)]) \times i\omega_i = 0 . \quad (4.4)$$

Collecting real and imaginary parts, the imaginary part of the equation requires that

$$\gamma = -\omega_i = \frac{Im[K_L(\omega_r)]}{\partial Re[K_L]/\partial \omega_r} , \quad (4.5)$$

where all terms are evaluated at  $\omega_r$ .

More concrete progress can be made by returning to equation (3.23) for the dielectric tensor  $K_{ij}(\omega, \mathbf{k})$  and the expressions (3.25) and (3.26) for  $K_L$  and  $K_T$ . Specifically we use the Plemelj formula to transform the resonant denominator  $(\omega - \mathbf{k} \cdot \mathbf{v})$  into two parts, the imaginary part of which involves a delta function:

$$\frac{A(\mathbf{v})}{(\omega - \mathbf{k} \cdot \mathbf{v} + i0)} = P \frac{A(\mathbf{v})}{(\omega - \mathbf{k} \cdot \mathbf{v})} - i\pi \delta(\omega - \mathbf{k} \cdot \mathbf{v}) , \quad (4.6)$$

where  $P$  denotes the Cauchy principal value of the integral. The delta function is then trivial to implement in (3.23), (3.25), and (3.26), leading to results like

$$ImK_L(\omega, \mathbf{k}) = \pi \sum_{\alpha} \frac{\omega_{p\alpha}^2}{\omega^2 V^2} \omega \left( \frac{\mathbf{k} \cdot \mathbf{v}}{k} \right)^2 \frac{\exp(-v_{\phi}^2/2V^2)}{(2\pi)^{3/2} V^3} \quad (4.7)$$

$$\propto \sum_{\alpha} \frac{\partial f_{\alpha}^0(v_{\phi})}{\partial v}. \quad (4.8)$$

Note that the expression depends on the slopes of the particle distribution functions evaluated at the phase velocity  $\mathbf{v}_{\phi} = v_{\phi} \mathbf{k}/k = \omega \mathbf{k}/k^2$  of the wave. Put another way, the expression depends on the relative numbers of particles moving faster or slower than  $v_{\phi}$ , as in Sectin 4.2's qualitative description of resonant wave growth and damping.

An important qualitative point is that this description of damping is “linear”, meaning that it depends on the perturbations  $f^1(\mathbf{v})$  of the distribution function that are linear in  $\mathbf{E}$  - see equation (3.19). Nonlinear damping comes from the higher order terms, proportional to  $E^2$  etc. Such processes are touched on in Section 4.5 and 4.7 below.

### 4.3.1 Landau damping of Langmuir waves

The temporal damping rate for Langmuir waves  $\gamma_L(\mathbf{k})$  is defined so that the wave energy varies with time as  $\exp(-\gamma_L(\mathbf{k})t)$ . Collecting results from the previous lecture for a Maxwellian electron distribution and substituting into the previous equation leads, via the last three equations to

$$\gamma_L(\mathbf{k}) = \left( \frac{\pi}{2} \right)^{1/2} \frac{\omega_L^4(\mathbf{k})}{k^3 V_e^3} \exp \left( -\frac{\omega_L^2(\mathbf{k})}{2k^2 V_e^2} \right). \quad (4.9)$$

Here  $\omega_L(\mathbf{k}) = (\omega_p^2 + 3k^2 V_e^2)^{1/2}$  is the Langmuir wave dispersion relation. Figure 4.3 illustrates the dispersion relation and the Landau damping rate for Langmuir waves. Note that ion effects can be included but are generally negligible for Langmuir waves. Landau damping becomes insignificant at high wave phase speeds (or equivalently, for low  $k$ ), where there are few electrons to resonantly accelerate. Weakly damped Langmuir waves (with  $\gamma_L/\omega_p \ll 1$ ) have frequencies close to the plasma frequency.

### 4.3.2 Landau and cyclotron damping of transverse waves

The dispersion relation for unmagnetized transverse waves is

$$\omega^2 = \omega_p^2 + k^2 c^2. \quad (4.10)$$

The phase speed thus satisfies  $v_{\phi}(k) = (\omega_p^2/k^2 + c^2)^{1/2} > c$ . For this reason there is no resonance between particles and waves (particles cannot travel faster than the speed of light) and Landau damping does not occur.

On the other hand, magnetized transverse waves ( $x$ -mode and  $o$ -mode waves) may be damped by a form of collisionless damping analogous to Landau damping referred to as cyclotron damping. The reason is that for magnetized plasmas the resonance condition between particles and waves becomes

$$\omega - k_{\parallel} v_{\parallel} - \frac{s\Omega_{\alpha}}{\gamma} = 0 \quad (4.11)$$

where  $\gamma$  is the Lorentz factor of the particle,  $\Omega_{\alpha}$  is the cyclotron frequency, and  $k_{\parallel}$ ,  $v_{\parallel}$  are the components of  $\mathbf{k}$  and  $\mathbf{v}$  parallel to  $\mathbf{B}$ . The resonance condition may be

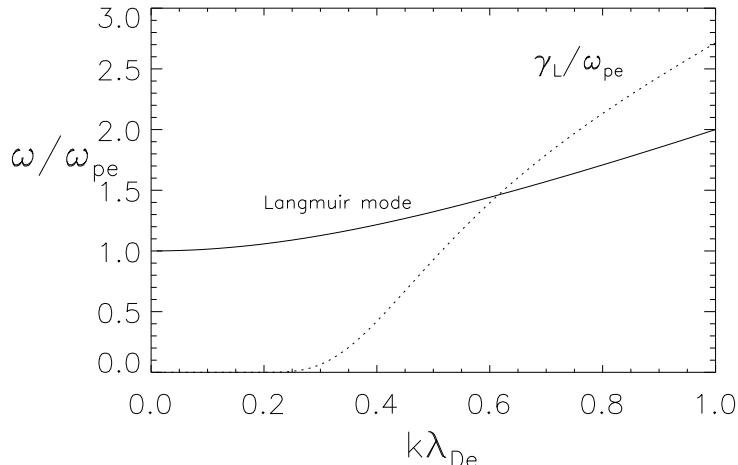


Figure 4.3: The dispersion relation (solid line) and Landau damping rate (dashed line) for Langmuir waves.

interpreted in the following way: in the reference frame where  $v_{\parallel}$  is zero, the wave frequency is equal to an integer multiple ( $s$ ) of the particle’s relativistic cyclotron frequency. For positive harmonic number  $s$ , waves with phase speeds greater than the speed of light can resonate with particles with  $v < c$ , due to the compensatory effect of the negative final term in equation (4.11). Negative cyclotron damping, where wave growth occurs in the  $x$ -mode or  $o$ -mode due to a positive slope in the distribution function is also known as *electron cyclotron maser emission* (see Lectures 17 and 18 for examples).

#### 4.4 Langmuir growth via an electron bump-in-tail instability

As explained in Section 4.2, wave growth can occur via negative or inverse Landau damping if there is a positive slope in the distribution function at velocities close to the phase velocity of the wave. An example of this is the growth of Langmuir waves via a “bump-in-tail instability”, one of many types of plasma instability in space plasmas. Such a situation occurs when the particle distribution function consists of three components, two for electrons and one for ions: background electrons with a Maxwellian distribution (number density  $n_0$  and thermal width  $V_0$ ), an electron beam described using a displaced Maxwellian (number density  $n_b$ , mean beam velocity  $v_b$ , and thermal width  $V_b$ ), and background ions with a Maxwellian distribution function. The primary role of the ions is to provide a charge-neutralizing background. This scenario is illustrated in Figure 4.2. Typically the beam number density satisfies  $n_b \ll n_0$ . To ensure that the beam is not swamped by the tail of the Maxwellian distribution, typically the condition  $v_b \gg V_0$  must be satisfied.

The dispersion equation now contains contributions corresponding to each particle component, although the ion contributions can typically be neglected for Langmuir waves. Carrying through the analyses the growth rate can be written in the form

$$\gamma(\mathbf{k}) = -\frac{\pi\omega^3(\mathbf{k})}{n_0k^2} \sum_{\alpha} \int d^3\mathbf{v} \mathbf{k} \cdot \frac{\partial f_{\alpha}(\mathbf{v})}{\partial \mathbf{v}} \delta(\omega(\mathbf{k}) - \mathbf{k} \cdot \mathbf{v}) \quad (4.12)$$

where  $\alpha$  corresponds to the three components. The argument of the delta function is the resonance condition, so that the integrand is non-zero only when the resonance condition  $\omega(\mathbf{k}) - \mathbf{k} \cdot \mathbf{v} = 0$  is satisfied. A necessary condition for wave growth is that

$$\left. \frac{\partial f_b(\mathbf{v})}{\partial \mathbf{v}} \right|_{\omega(\mathbf{k}) - \mathbf{k} \cdot \mathbf{v} = 0} > 0. \quad (4.13)$$

In Figure 4.2 this condition is satisfied for wave phase speeds in the range  $v_b - V_b \lesssim v_\phi \cos \theta \lesssim v_b$ , corresponding to the positive slope in the distribution function on the low-velocity side of the beam.

Note that the waves grow only if the growth rate due to the beam (the negative of the damping rate) exceeds the sum of the damping rates due to the wave's resonant interactions with the other particle components. Realistic situations involve competition between growth and damping.

What happens to the particle distribution as the waves grow? Obviously, the energy of the resonant particles must decrease, thereby increasing the number of particles at low  $v < v_\phi$  and decreasing the number at high  $v > v_\phi$ . The result is that the positive slope of the beam is reduced and the growth rate becomes smaller. The beam thus tends towards a plateau distribution, illustrated in Figure 4.4, in which the growth rate is zero and the beam has been flattened and extended to low speeds (ideally zero). Similarly, the wave energy increases smoothly, albeit at an increasingly slower rate, until it saturates at a maximum value. This process is called *quasilinear relaxation* and a state in which the particle distribution function leads to zero growth rate is said to be *marginally stable*.

Quasilinear relaxation is the back-reaction to the wave growth, tending to limit the loss of particle energy to the waves and so the wave amplitude. Analogues exist for essentially any wave instability and the particle distribution that drives the waves.

## 4.5 Burstiness of waves: SGT and other theories

Quasilinear relaxation and thermal damping tend to reduce the growth rate of an instability and cause the particle distribution to evolve towards marginal stability, for which the waves encounter no net growth or damping. In space waves typically grow in bursts with widely varying energy densities. What causes these bursts?

Moreover, electron beams and unstable particle distributions typically persist for much greater distances than predicted on the basis of quasilinear theory. For instance, the electrons that produce type III solar radio bursts, discussed in the next section, should be quasilinearly plateaued within 100 km of their source yet are observed to propagate to 1 AU.

Nonlinear processes can also cause waves to grow in bursts, for instance by nonlinear self-focusing or modulational instabilities. They can also limit the growth of waves (e.g., Langmuir waves) by transferring energy into product waves that are damped. Examples are given in Section 4.7 below. Nonlinear processes can also prevent quasilinear relaxation from proceeding to completion, thereby preserving the particle distribution function in an unstable or marginally stable state. However, they only work when the wave level exceeds a threshold, different for the specific instability and nonlinear process under consideration.

An alternative is to relax the assumption that the medium is homogenous and to consider the effect on the unstable particle distribution of propagation through an inhomogenous plasma (Figure 4.5). Specifically, in regions where the plasma inhomogeneity favours growth (e.g., the growth rate is larger), then the waves will grow more and quasilinearly push the particle distribution towards marginal stability. Regions where the growth is or is not favoured will then inject fluctuations into

the particle distribution, tending to break it up and introducing time variability. Under certain circumstances the particle distribution tends to reform (e.g., due to fast particles outrunning slow ones and reforming a beam) and so a steady state can be built up in which there is competition between destruction of the unstable particle distribution in growth sites and re-formation between growth sites and the overall state is near marginal stability. In this case the unstable particle distribution can persist and the wave growth will be bursty. Time and volume-averaged the net growth rate can be close to zero, with time-localized fluctuations in the particle distribution leading to bursty wave growth and damping.

This theory, developed here at the University of Sydney, is called Stochastic Growth Theory (SGT). The reason for the name is that time-varying wave field  $E = E(t)$  can be written

$$E(t) = E_0 e^{\int_{-\infty}^t dt \gamma} = E_0 \exp\left(\sum \Delta G\right). \quad (4.14)$$

Accordingly the wave gain  $G(t) = \int_{-\infty}^t dt \gamma$  can be written as the sum of fluctuations  $\Delta G$ . Then, provided only that many  $\Delta G$  cross a growth site during the time a packet of waves is there, then the Central Limit Theorem requires that  $G$  be a Gaussian random variable (or stochastic variable). This means that the statistics of the probability distribution of wave electric fields should be lognormal. Put another way, the statistics of the bursty wave fields should have a definite functional form.

Multiple comparisons between solar system plasma waves and SGT show that SGT is widely applicable for multiple wave modes (both electrostatic and electromagnetic), multiple sources of particle free energy (electron beams and ion temperature anisotropies), and multiple contexts (type III solar radio bursts to foreshock regions, magnetosheaths, and magnetospheric plasmas). An example is shown in Figure 4.6. Even normal pulsar radio emissions have been shown to be consistent with SGT.

SGT is not always applicable. Empirically, not all bursty waves show the lognormal field statistics predicted by SGT. For instance, some solar and Jovian radio emissions, as well as giant pulses from pulsars, appear to show power-law statistics.

Thus, while “complex system” theories for wave growth appear very attractive in multiple contexts, dealing with self-consistent wave-particle coupling in inhomogenous plasmas, there is scope for other processes too. Nonlinear processes, for instance, can coexist with SGT. At other times it is likely that nonlinear processes will dominate.

## 4.6 Type III solar radio bursts

Type III solar radio bursts are generated by fast electron beams accelerated by solar flares. The electron beams propagate out into the solar wind along interplanetary magnetic field lines (the Parker spiral) with typical speeds  $v_b \approx (0.1 - 0.3)c$ . Langmuir waves are generated via the bump-in-tail instability near the resonant wavenumber  $k_b \approx \omega_p/v_b$ . Radio emission at  $\omega_p$  and  $2\omega_p$  is subsequently generated through nonlinear wave-wave processes involving the beam-driven Langmuir waves (see Section 4.7). An example of a type-III-associated beam measured in situ by a spacecraft is shown in Figure 4.7, where only part of the tail of the thermal electron distribution is visible. The electron distribution function in Figure 4.7 exhibits a positive slope over the range of velocities:  $v_- < v_{\parallel} < v_+$ . The propagation path of the electron beam may be traced by following the source of the radio emissions. This is illustrated in Figure 4.8, where the radio source is tracked using triangulation methods from two spacecraft (WIND in the ecliptic plane and Ulysses above the ecliptic plane). Note that the radio emission frequency decreases as the type

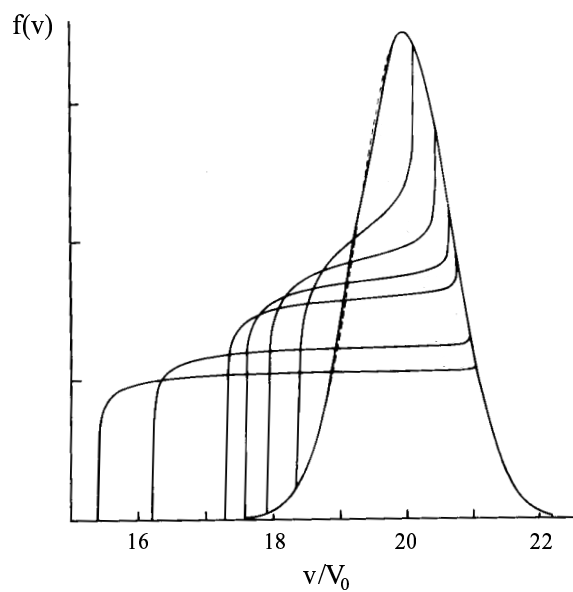


Figure 4.4: Results from a simulation demonstrating quasilinear relaxation of an originally Maxwellian beam to a plateau distribution (Grognard, 1975). The thermal Maxwellian component is not shown. The mean beam velocity  $v_b = 20V_0$  and the beam thermal velocity  $V_b = V_0$ .

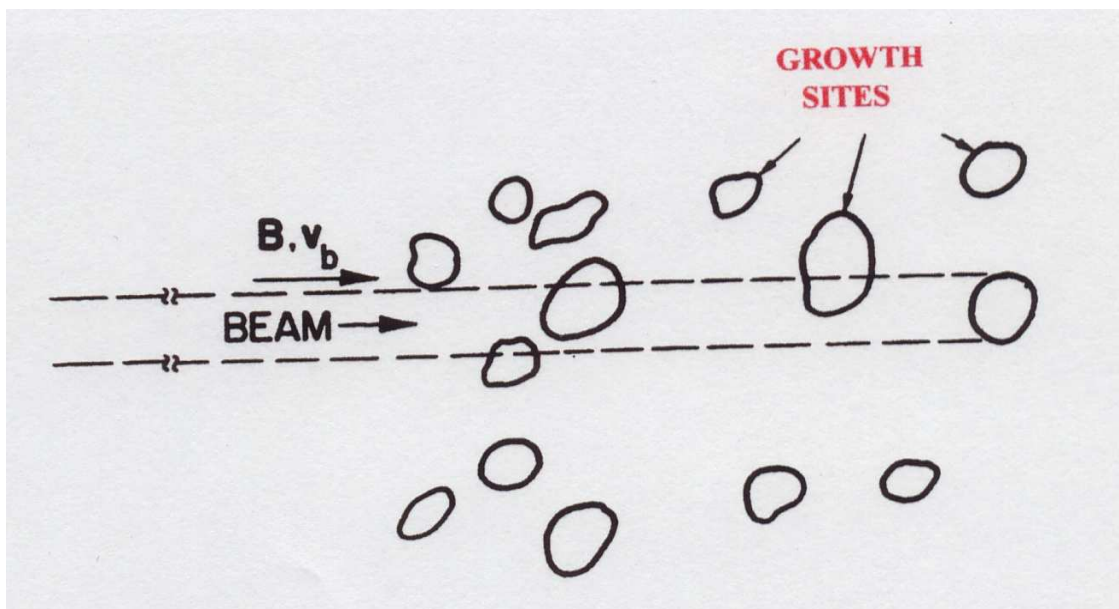


Figure 4.5: Propagation of a beam through an inhomogeneous plasma.

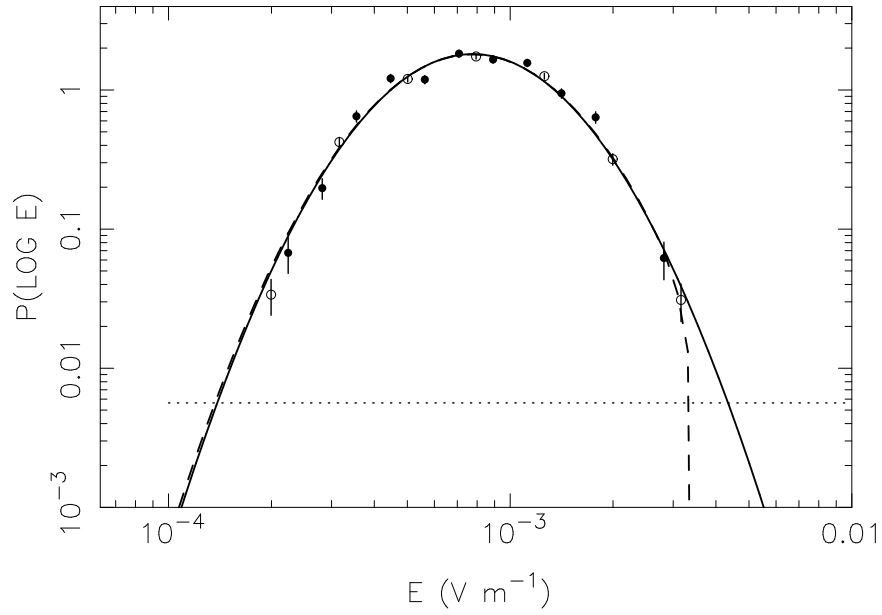


Figure 4.6: Comparison of observational data with SGT for Langmuir waves in Earth's magnetosphere, above Earth's polar cap [Cairns and Menietti, 2001].

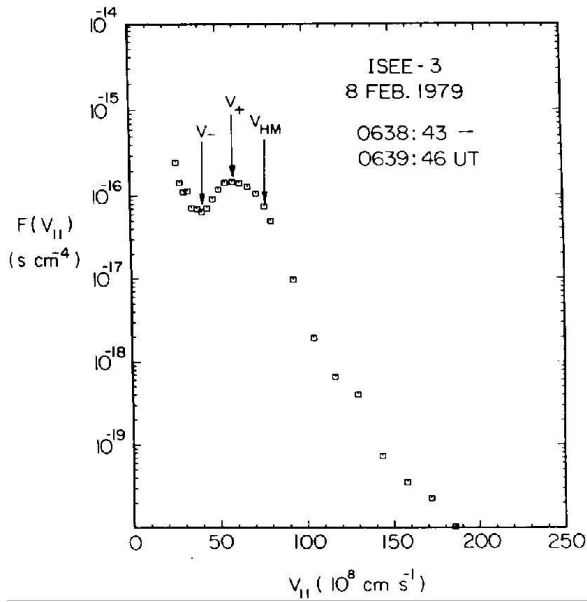


Figure 4.7: Reduced electron distribution function (parallel to  $\mathbf{B}$ ) with a type III beam measured in interplanetary space by the ISEE 3 spacecraft (from Cairns and Robinson, 1995).

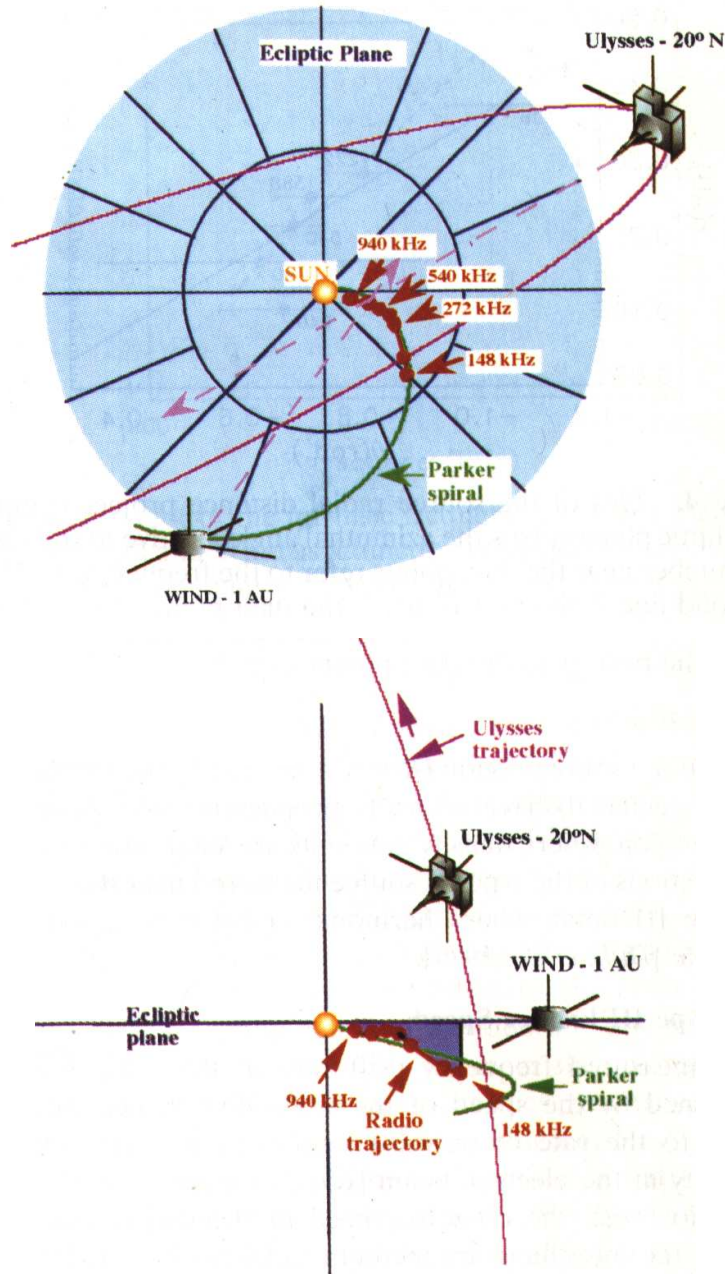


Figure 4.8: Trajectory of a type III radio source using triangulation with the WIND and Ulysses spacecraft (Reiner *et al.*, 1998). The top view is projected onto the ecliptic plane. The bottom view is projected onto a plane perpendicular to the ecliptic plane.

III beam propagates away from the Sun. This is because the radio emission is generated at the plasma frequency (or  $2\omega_p$ ), which decreases with decreasing plasma density away from the Sun.

Figure 4.9 shows the dynamic spectrum of a sequence of type III bursts observed by the WIND spacecraft. One type III burst in this sequence commences near 11:00 hours at frequencies  $\approx 1$  MHz and rapidly drops to frequencies of tens of kHz. We know that the electron beam associated with this particular type III burst reaches the spacecraft (local plasma frequency  $\approx 25$  kHz at the spacecraft) because Langmuir waves are observed in situ, commencing at  $\approx 11:45$  (see bottom panel). Electron beams ejected from an active region on the Sun typically have a spread in velocities  $\Delta v_b/v_b \approx 0.1 - 0.3$ . Therefore the spatial extent of the beam increases as it propagates out from the Sun. Consequently, with decreasing frequency (corresponding to increasing distance from the Sun) the duration of a type III burst increases, as is evident in Figure 4.9.

An analogue to Figure 4.6 shows that the Langmuir waves associated with Type III bursts are consistent with SGT [Robinson et al., 1993]. In this case, the observed field statistics have a parabolic form, as well as evidence for a nonlinear process limiting the distribution at the highest fields.

Figure 4.10 shows a coronal type III burst, which displays simultaneous radio emission at  $\omega_p$  and  $2\omega_p$ . The most widely accepted explanation for the generation of radio emission in type III bursts involves *nonlinear wave-wave processes*, as discussed in the next section. Electron beams in the corona may also be accelerated towards the Sun, with the result that the frequency of the type III burst increases with time.

## 4.7 Nonlinear wave-wave processes

Type III bursts are detected remotely in the form of radio emissions (i.e., waves in the  $x$  or  $o$ -modes). Langmuir waves cannot escape from the source region, because as they propagate into decreasing plasma densities, they shift to higher wavenumbers where they undergo significant Landau damping (see Figure 4.3). In this Section, one mechanism to convert Langmuir waves to observable  $x$  and  $o$ -mode waves is discussed.

Up to now we have considered only the linear response of the plasma to electromagnetic fields (for instance, in the derivation of the general wave equation). If the next highest order terms are retained ( $\propto E^2$ ), the relation between the current density  $\mathbf{J}$  and the electric field  $\mathbf{E}$  can be expressed in the form

$$\begin{aligned}
 J_i(\omega, \mathbf{k}) &= \sigma_{ij}(\omega, \mathbf{k})E_j(\omega, \mathbf{k}) + \int \frac{d\omega' d^3\mathbf{k}' d\omega'' d^3\mathbf{k}''}{(2\pi)^4} \sigma_{ijk}(\omega, \omega', \omega'', \mathbf{k}, \mathbf{k}', \mathbf{k}'') \\
 &\times E_j(\omega', \mathbf{k}')E_k(\omega'', \mathbf{k}'')\delta(\omega - \omega' - \omega'')\delta(\mathbf{k} - \mathbf{k}' - \mathbf{k}''). \quad (4.15)
 \end{aligned}$$

The second term describes the quadratic nonlinear response of the plasma, which is the response to the combined effects of two different fields  $\mathbf{E}(\omega', \mathbf{k}')$  and  $\mathbf{E}(\omega'', \mathbf{k}'')$ . This second order current acts as a source for another field with frequency  $\omega$  and wavevector  $\mathbf{k}$ . Another way of looking at this is that two waves with frequency and wavevector  $(\omega', \mathbf{k}')$  and  $(\omega'', \mathbf{k}'')$  beat together to produce a new wave at  $(\omega, \mathbf{k})$ . Such wave-wave interactions must obey both frequency and wavevector conservation (corresponding to the arguments of both the delta functions in equation (4.15) being equal to zero), with

$$\omega' + \omega'' = \omega, \quad (4.16)$$

and

$$\mathbf{k}' + \mathbf{k}'' = \mathbf{k}. \quad (4.17)$$

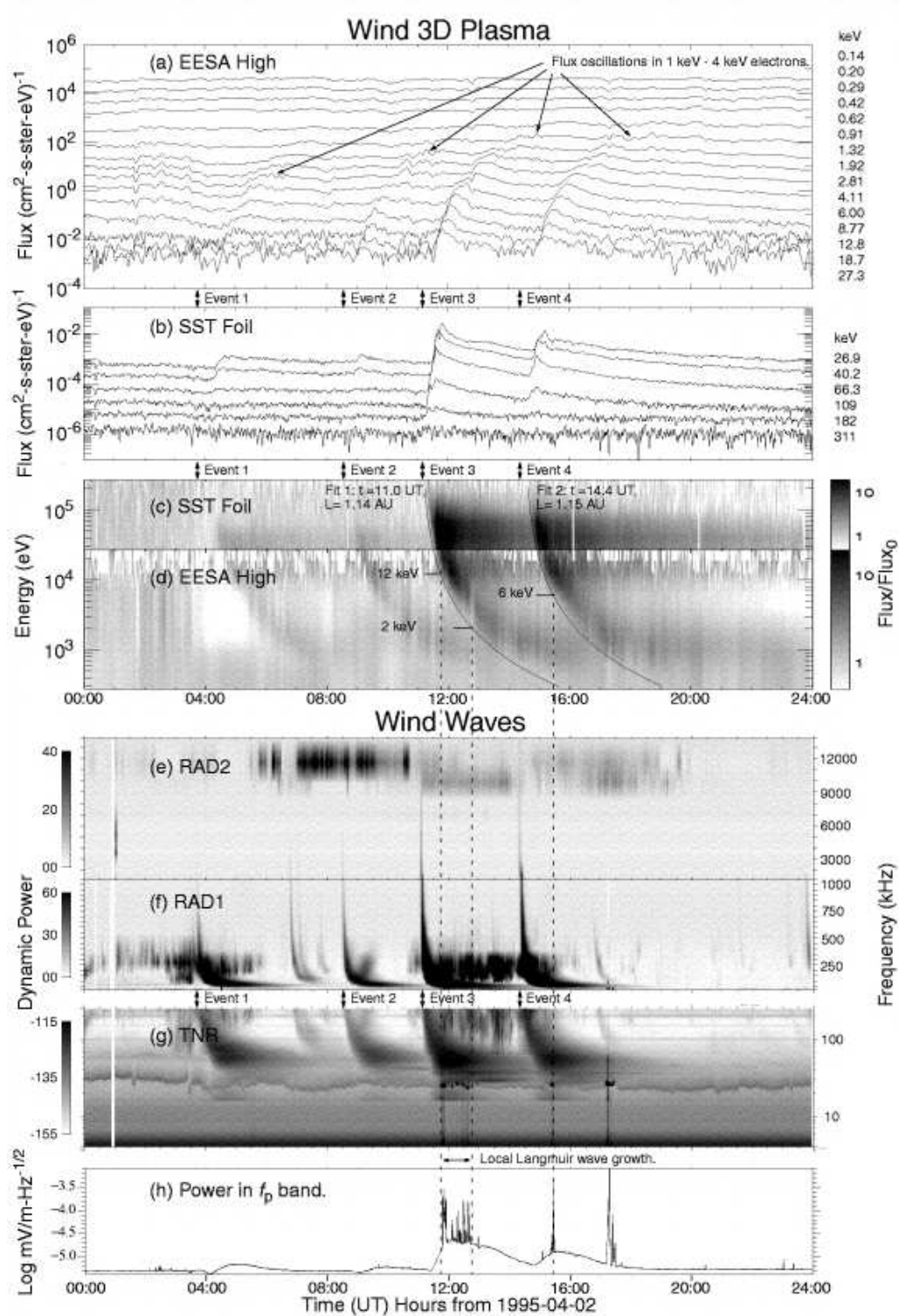


Figure 4.9: WIND observations of interplanetary type III radio bursts (Ergun *et al.*, 1998). The various panels correspond to: (a-b) Electron fluxes at various energies, (c-d) spectrograms of the relative change in electron flux, (e-g) dynamic spectra (wave power plotted as wave frequency versus time) (h) wave power at the local plasma frequency, where the rapid variations in power correspond to bursty Langmuir waves.

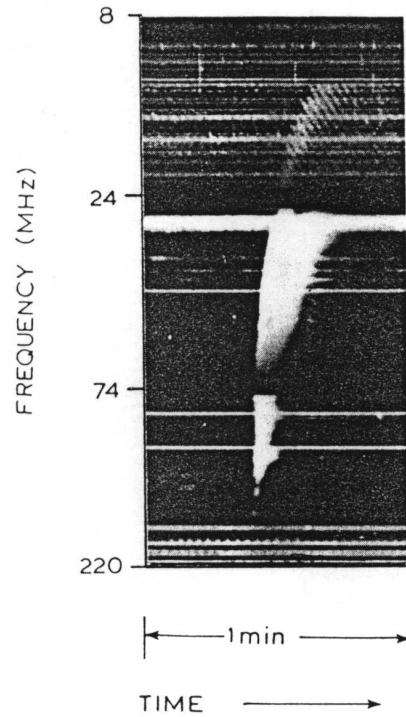


Figure 4.10: Dynamic spectrum of a coronal type III burst with fundamental and harmonic components (Suzuki and Dulk, 1985).

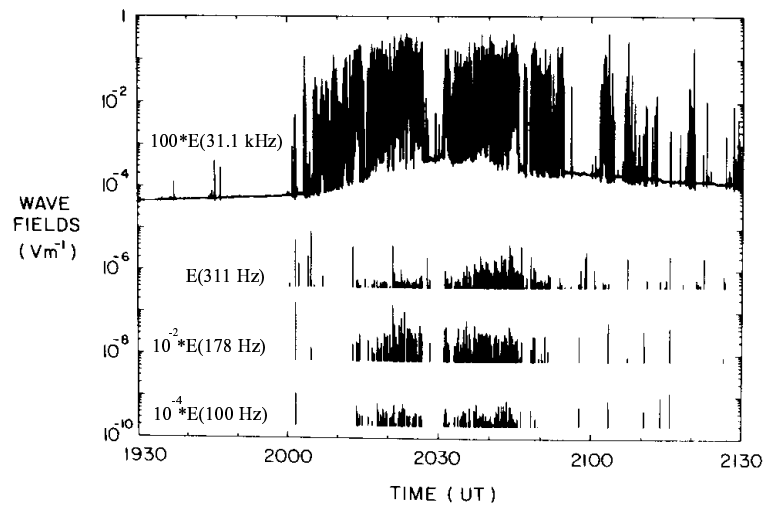


Figure 4.11: Wave fields measured during a type III event by the ISEE 3 spacecraft. Intense Langmuir waves and radio emission (smooth emissions commencing after 2000 UT) are detected in the high frequency channel (31.1 kHz). The bursty waves in the lower frequency channels (with background level removed) are ion sound waves (Cairns and Robinson, 1995).

The *kinematic conditions* for a wave-wave process to proceed are that (4.16) and (4.17) are satisfied and that  $\omega$  and  $\mathbf{k}$  for each wave satisfies the dispersion relation for the relevant wave mode.

Three nonlinear wave-wave processes are involved in generating type III radiation at  $\omega_p$  and  $2\omega_p$ . The first process is *electromagnetic decay* ( $L \rightarrow T + S'$ ), where a beam-driven Langmuir wave  $L$  decays into a transverse electromagnetic wave  $T$  ( $x$  or  $o$ -mode wave) and a low frequency ion sound wave  $S'$ . Frequency conservation (equation (4.16)) implies that  $\omega_T \approx \omega_{pe}$  (corresponding to fundamental emission). Radiation at the second harmonic is generated via a two-stage process: (i) *Electrostatic decay* ( $L \rightarrow L' + S$ ), where a beam-driven Langmuir wave  $L$  decays into a daughter Langmuir wave  $L'$  and an ion sound wave  $S$ . The product Langmuir waves are backscattered in this process; i.e., their wavevectors point in the opposite direction to the beam-driven Langmuir waves  $L$ . (ii) *Langmuir wave coalescence* ( $L + L' \rightarrow T'$ ), where beam-driven and backscattered Langmuir waves coalesce to produce  $x$  or  $o$ -mode waves at  $2\omega_p$ . The existence of a backscattered population of Langmuir waves (from electrostatic decay) is necessary for second harmonic radiation to be generated.

Strong evidence that such processes do indeed occur was provided by the ISEE-3 spacecraft, which detected high wave levels in low frequency channels, consistent with ion sound waves, which correlate with the intense Langmuir waves and radio emission in type III events, as shown in Figure 4.11.

## Further reading:

1. Cairns, I. H., and J. D. Menietti, 2001, Stochastic growth of waves over Earth's polar cap, *J. Geophys. Res.*, **106**, 29,515.
2. Cairns, I. H., and Robinson, P. A., 1995, Ion acoustic wave frequencies and onset times during type III solar radio bursts, *Astrophys. J.*, **453**, 959.
3. Cairns, I.H., S. Johnston, and P. Das, 2001, Intrinsic variability of the Vela pulsar: Log-normal statistics and theoretical implications, *Astrophys. J.*, **563**, L65.
4. Ergun, R. E. *et al.*, 1998, WIND spacecraft observations of solar impulsive electron events associated with solar type III radio bursts, *Astrophys. J.*, **503**, 435.
5. Grogard, R. J.-M., 1975, Deficiencies of the asymptotic solutions commonly found in the quasilinear relaxation theory, *Aust. J. Phys.*, **28**, 731.
6. Melrose, D. B., 1986, *Instabilities in space and laboratory plasmas*, Cambridge University Press, Cambridge.
7. Reiner, M. J., Fainberg, J., Kaiser, M. L., and Stone, R. G., 1998, Type III radio source located by Ulysses/Wind triangulation, *J. Geophys. Res.*, **103**, 1923.
8. Robinson, P.A., B. Li, and I.H. Cairns, New regimes of stochastic wave growth, *Phys. Rev. Lett.*, **93**, 235003-1 (4 pages), 2004.
9. Robinson, P. A., Cairns, I. H. and Willes, A. J., 1994, Dynamics and efficiency of type III solar radio emission, *Astrophys. J.*, **422**, 870.
10. Suzuki, S. and Dulk, G. A., 1985, Bursts of Type III & Type V, in *Solar Radiophysics*, eds: D. J. McLean and N. R. Labrum, Cambridge: Cambridge University Press, Chapter 12.